atmosphere

MDPI

Article

Transport Pathways and Potential Source Regions of $PM_{2.5}$ on the West Coast of Bohai Bay during 2009–2018

Tianyi Hao [1], Ziying Cai [2], Shucheng Chen [3], Suqin Han [1,*], Qing Yao [1] and Wenyan Fan [2]

[1] Department of Environmental Meteorological Assessment, Tianjin Environmental Meteorological Center, No. 100 Qi Xiang Tai Road, Tianjin 300074, China; haotianyi11@163.com (T.H.); yao.qing@163.com (Q.Y.)
[2] Department of Environmental Meteorological Forecast, Tianjin Environmental Meteorological Center, No. 100 Qi Xiang Tai Road, Tianjin 300074, China; 120078030@163.com (Z.C.); fwy210@163.com (W.F.)
[3] Department of Technical Support, Tianjin Meteorological Observation Center, No. 62 Friendship Road, Tianjin 300061, China; csc18780007860@163.com
* Correspondence: zhafox@nankai.edu.cn

Received: 29 May 2019; Accepted: 20 June 2019; Published: 25 June 2019

Abstract: Mass concentration data for particulate matter with an aerodynamic diameter less than or equal to 2.50 μm ($PM_{2.5}$) combined with backward trajectory cluster analysis, potential source contribution function (PSCF), and concentration weighted trajectory (CWT) methods were used to investigate the transport pathways and potential source regions of $PM_{2.5}$ on the west coast of Bohai Bay from 2009 to 2018. Two pathways responsible for the transportation of high $PM_{2.5}$ levels were identified, namely a southerly pathway and a northwesterly pathway. The southerly pathway represented the major transport pathway of $PM_{2.5}$ for all seasons. As a regional transport pathway, it had the greatest impact in winter, followed by autumn. The southerly transport pathway passed over the Shandong and Hebei provinces before reaching Tianjin: Air masses were transported within the boundary layer (below 925 hPa), representing a slow-moving air flow. The northwesterly pathway mostly occurred in winter and autumn and passed over desert and semidesert regions in Outer Mongolia, the sand lands of Inner Mongolia, and Hebei. The air masses associated with the northwesterly pathway represented fast-moving airflows responsible for long-range transportation of $PM_{2.5}$. Two potential source regions that contributed to high $PM_{2.5}$ loadings on the west coast of Bohai Bay were identified, "southerly source regions" and "northwesterly source regions". The southerly source regions, with weighted CWT (WCWT) values in winter greater than 140.00 μg/m^3, were anthropogenic source regions, including southern Hebei, western Shandong, eastern Henan, northern Anhui, and northern Jiangsu. The northwesterly source regions, with WCWT values in winter of 80.00–140.00 μg/m^3, were natural source regions, encompassing central Inner Mongolia and southern Mongolia. In addition, the southerly transport pathway passed though anthropogenic source regions, while the northwesterly transport pathway passed though natural source regions. The impacts of anthropogenic source regions on $PM_{2.5}$ loadings on the west coast of Bohai Bay were greater than those of natural source regions.

Keywords: backward trajectory; transport pathway; potential source region; $PM_{2.5}$; west coast of Bohai Bay

1. Introduction

Due to rapid economic development and urbanization in the past few decades, there has been an escalating increase in energy consumption in China, with a corresponding deterioration of air quality [1]. The term "complex atmospheric pollution" has emerged in the last decade, because

atmospheric pollutants in China are complex mixtures of various sources [2]. One of the major air pollutants is particulate matter (PM), particularly $PM_{2.5}$ (with an aerodynamic diameter less than or equal to 2.50 μm), which remains a nationwide problem despite considerable abatement efforts. Beijing–Tianjin–Hebei is the most prominent area of air pollution in China [3]. Further, $PM_{2.5}$ is also the major air pollutant in Beijing–Tianjin–Hebei [4]. The long-range transport of particulate matter adds to locally emitted $PM_{2.5}$, increasing the ambient concentrations of $PM_{2.5}$ and therefore exacerbating human health effects [5–7]. Effective $PM_{2.5}$ control strategies require knowledge of transportation and source regions of $PM_{2.5}$. $PM_{2.5}$ concentrations on the west coast of Bohai Bay also are often elevated abnormally and rapidly because of transportation, especially in winter and autumn. It is therefore important to determine transport pathways and potential source regions of $PM_{2.5}$.

The regional transportation and source regions of PM have been of increasing concern in the last two decades [8–12]. It is an indisputable fact that PM is transported across regions [13,14]. The regional transportation of PM depends on meteorological conditions, topography, and emissions sources. The sources of atmospheric pollutants in China are complicated and various, and they include anthropogenic and natural sources, primary and secondary sources, and local and regional sources [15]. Wang et al. [16] used trajectory clustering and a potential source contribution function (PSCF) to identify three principal transport pathways for high concentrations of PM_{10} in Beijing during springtime from 2001 to 2003. A similar analysis in XiAn was also performed by them [17]. In addition, a comparison between the dust sources affecting Beijing and XiAn showed that northwesterly sources are more important for XiAn, and arid and semiarid regions in Mongolia are more important for Beijing. Xin et al. [18] used 3D cluster analysis and a PSCF to identify the long-range transport pathways and potential sources of PM_{10} in the Tibetan Plateau uplift area and found that a seasonal variation of transport pathways and contributions from sources outside Xining were significant in spring and winter. Zhu et al. [19] held that four transport pathways of high PM_{10} exist in Beijing based on backward trajectories and PM_{10} concentration records from 2003 to 2009. Both natural sources of dust and sand in southern Mongolia and western Inner Mongolia and anthropogenic sources in Shanxi and Hebei had significant impacts on the high concentrations of PM_{10} in Beijing. During 2009–2012, the regional contributions of PM_{10} from Shandong, Tianjin, and Henan increased, whereas those from Inner Mongolia and Mongolia decreased compared to 2003–2009 [20]. The highest concentrations of $PM_{2.5}$ in Beijing were associated with southern, southeastern, and short-north trajectories. In addition, the annual mean contribution of 35.50% $PM_{2.5}$ was attributed to long-distance transportation during 2005–2010 [21]. Wang et al. [16] suggested that the transport pathways corresponding to the highest daily average concentrations of PM_{10} and NO_2 for Tianjin were concentrated in the northwest airflow from inland areas in winter, spring, and autumn. Further, Tianjin, Hebei, and Shandong were the major local potential source regions of these two pollutants. However, little work focused on transport pathways and potential source regions of $PM_{2.5}$ has been done on the west coast of Bohai Bay.

Back trajectory analysis is a powerful tool for establishing the spatial domain of air parcels arriving at receptor sites. Statistical methods such as trajectory clustering, PSCFs, and CWT have been widely used to identify the pathways and sources of air pollution [22–24]. Moody and Galloway [25] were the first to exploit trajectory coordinates as clustering variables, and various other clustering algorithms have been developed in recent studies [26,27]. A PSCF is a simple but effective method to investigate potential sources. This method tends to give good angular resolution but poor radial resolution because the trajectories converge as they approach the receptor [28]. The method combining concentrations developed by Seibert et al. [29] calculates the geometric mean concentration of each grid cell, which is then weighted by the residence time. Stohl [30] refined this method by redistributing the concentration fields, and Hsu et al. [31] further refined it into a CWT method.

The objective of this research was to investigate the transport pathways and potential sources of $PM_{2.5}$ on the west coast of Bohai Bay on the basis of seasons from 2009 to 2018. $PM_{2.5}$ pollution transport pathways were analyzed based on back trajectory cluster analysis. Furthermore, potential $PM_{2.5}$ source regions were determined through both the PSCF and CWT methods. Finally, the results

provided through the PSCF and CWT methods were compared to China's anthropogenic $PM_{2.5}$ emissions inventory.

2. Material and Methods

2.1. Site Location and Data

The area of interest in this study is located on the west coast of Bohai Bay (39°06′ N, 117°10′ E) (Figure 1). The land slopes downwards gradually from northwest to southeast. Tianjin is confined by Taihang Mountain to the west, the Bohai Sea to the east, Yanshan Mountain to the north, and a plain to the south. It is one of the four municipalities of China and is one of the fast-growing economic megacities in the Beijing–Tianjin–Hebei urban agglomeration. Rapid economic development has resulted in an increase in the emissions of aerosol and a concomitant increase in aerosol levels in ambient air.

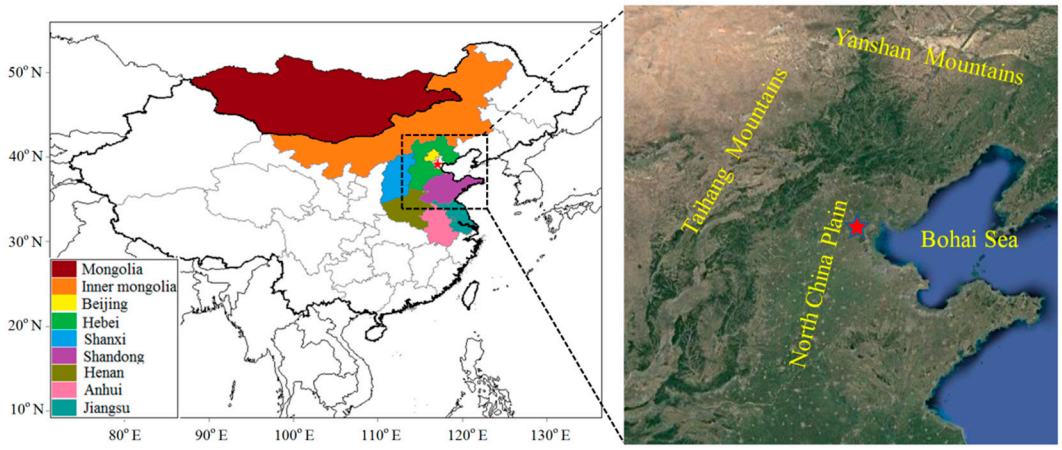

Figure 1. Location of the study area (the red star represents the west coast of Bohai Bay).

The hourly average $PM_{2.5}$ mass concentration data for Tianjin from January 2009 to February 2018 used in this study were obtained from the National Urban Air Quality Real-Time Publishing Platform (http://106.37.208.233:20035/) (January 2014–February 2018) and the Tianjin atmospheric boundary layer observation station (January 2009–December 2013). The $PM_{2.5}$ data from the National Urban Air Quality Real-Time Publishing Platform, which was released by the China National Environmental Monitoring Center, represented the average $PM_{2.5}$ levels in Tianjin. The mean $PM_{2.5}$ concentration values were computed from 13 state-controlled monitoring sites in Tianjin. The $PM_{2.5}$ concentration data released by the China National Environmental Monitoring Center began in 2014. In order to analyze the long-term characteristics of $PM_{2.5}$, the monitoring data from the Tianjin atmospheric boundary layer observation station of the China Meteorological Administration from 2009 to 2013 were combined. Both datasets were obtained from oscillating microbalance measurements. An equivalence trail was carried out between them from 2014 to 2016. The results of this trail were used to correct the $PM_{2.5}$ concentration data from 2009 to 2013.

The anthropogenic emissions $PM_{2.5}$ data from 2016 were from a multiresolution emissions inventory for China (http://www.meicmodel.org/dataset-meic.html). The spatially disaggregated anthropogenic emissions inventory grids emissions were from power generation, industry, residential heating, and transportation at a resolution of 0.50° × 0.50° latitude–longitude. The hourly wind speed and direction data used to create wind roses were obtained from the Tianjin Meteorological Service. In a meteorological sense, March to May, June to August, September to November, and December to February (the following year) were defined as spring, summer, autumn, and winter, respectively.

2.2. Backward Trajectory and Cluster Analysis

The individual 3D trajectories were calculated using NOAA HYSPLIT4.9 with Global Data Assimilation System (GDAS) meteorological data, which supplies 3-h, global 1° latitude–longitude datasets of the pressure surface. Seventy-two-hour back trajectories were calculated at 6-h intervals (00:00 h, 06:00 h, 12:00 h, and 18:00 h UTC) for every day in the period of interest, for an arrival height of 200 m. At a height of 200 m, particles are well mixed under various weather conditions [32], and elevated or degraded air masses could both reach the 200-m receptor height.

To explore the impact of air mass transport on $PM_{2.5}$, backward trajectories of air parcels were clustered using the Euclidean distance method based on the TrajStat software developed by Wang et al. [33]. The Euclidean distance method is often used to define the distance between two trajectories using latitude and longitude locations as variables. The "eyeball" method (Wang et al., 2009; Wang et al., 2015) is used to determine the cluster numbers in this software. In this analysis, a cluster number of 6 was decided. The 6 clusters provided the most appropriate representation of air mass classifications according to the "eyeball" method. Trajectories with $PM_{2.5} > 75.00$ μg/m^3 were considered to be polluted trajectories, which is China's national class II standard of $PM_{2.5}$ daily mean concentration [34].

2.3. Potential Source Contribution Function (PSCF)

Potential source regions of concentration back trajectories for $PM_{2.5}$ can be identified through a PSCF, which analyzes trajectory pathways [35–37] (Zeng and Hopke, 1989; Polissar et al., 1999; Begum et al., 2005). To calculate the PSCF, the whole geographic region covered by the trajectories is divided into an array of grid cells whose size is dependent on the domain of the back trajectories. The PSCF values for these grid cells are calculated by counting the trajectory segment endpoints that terminate within each cell. The number of endpoints that fall in the ijth cell are marked as n_{ij}. The number of endpoints in the ijth cell having the same arrival times at the sampling site corresponding to pollutant concentrations higher than an arbitrary criterion are denoted as m_{ij}. The PSCF value for the ijth cell is defined as

$$\mathrm{PSCF_{ij}} = \mathrm{m_{ij}}/\mathrm{n_{ij}} \tag{1}$$

The PSCF value can be interpreted as a conditional probability that describes the spatial distribution of probable source locations. Cells with high PSCF values are potential source areas and should coincide with a pollutant emissions region within the domain. These cells are indicative of areas of "high potential" for contributions to receptor site pollution. However, cells with low PSCF values do not indicate low emissions, because emissions may not be transported to the receptor site.

The PSCF grids cover a domain between 20 and 70° N and 75 and 130° E, with a 0.50° × 0.50° resolution. To reduce uncertainty in cells with small n_{ij} values, an arbitrary weight function W (n_{ij}) is multiplied into the PSCF value [38–41] (Polissar et al., 2001a,b; Karaca et al., 2009; Xu et al., 2010). Equation (2) was used to obtain the weight function in this study:

$$W_{ij} = \begin{cases} 1.00 & 80 < \mathrm{n}_{ij} \\ 0.70 & 20 < \mathrm{n}_{ij} \le 80 \\ 0.42 & 10 < \mathrm{n}_{ij} \le 20 \\ 0.05 & \mathrm{n}_{ij} \le 10 \end{cases} \tag{2}$$

At last, the WPSCF is expressed as

$$\mathrm{WPSCF} = W_{ij} \times \mathrm{PSCF} \tag{3}$$

2.4. Concentration Weighted Trajectory (CWT)

A limitation of the PSCF method is that grid cells could have the same PSCF value when sample concentrations are either only slightly higher or much higher than the criterion. As a result, it cannot distinguish strong sources from moderate ones. Therefore, CWT [17,29,30] was used in this study. CWT can more easily distinguish source strength by assigning the concentration values at the receptor site to their corresponding trajectories. In the CWT method, a grid is superimposed over the domain of trajectory computations. Each grid cell is assigned a residence-time-weighted concentration from the measured sample associated with the trajectories that crossed that grid cell, as follows:

$$C_{ij} = \frac{1}{\sum_{l=1}^{M} \tau_{ijl}} \sum_{l=1}^{M} c_l \tau_{ijl}, \quad (4)$$

where C_{ij} is the average weighted concentration in the ijth cell, l is the index of the trajectory, M is the total number of trajectories, C_l is the concentration observed on arrival of trajectory l, and τ_{ijl} is the time spent in the ijth cell by trajectory l. A high value for C_{ij} implies that air parcels traveling over the ijth cell are associated with high concentrations at the receptor.

To minimize the inaccuracy caused by the small number of polluted trajectories, arbitrary weight functions are needed to reduce uncertainty, and the empirical weight function W_{ij} for PSCF can also be used in the CWT method. The WCWT is defined as

$$\text{WCWT} = W_{ij} \times C_{ij}. \quad (5)$$

3. Results and Discussions

3.1. Variation in $PM_{2.5}$ Concentrations

Seasonal and annual variations of $PM_{2.5}$ concentrations from 2009 to 2018 in Tianjin are shown in Figure 2. The $PM_{2.5}$ time series shows that annual $PM_{2.5}$ levels varied between 68.41 and 67.88 μg/m^3 from 2009 to 2012, reaching their maximum value (79.51 μg/m^3) in 2013 and then declining steadily ever since. Throughout the whole study period, $PM_{2.5}$ levels exceeded the class II standard of the Chinese National Air Quality Standards (75.00 μg/m^3) [34] and exhibited considerable seasonal variations. On average, high $PM_{2.5}$ concentrations in Tianjin always occurred in the winter, followed by autumn and spring, then summer. The mean concentrations and concentrations above the 75th percentile were higher in winter than in the other three seasons. The highest winter mean $PM_{2.5}$ concentration (109.98 μg/m^3) was observed in 2016, while the lowest winter mean value of 57.20 μg/m^3 was observed in 2017.

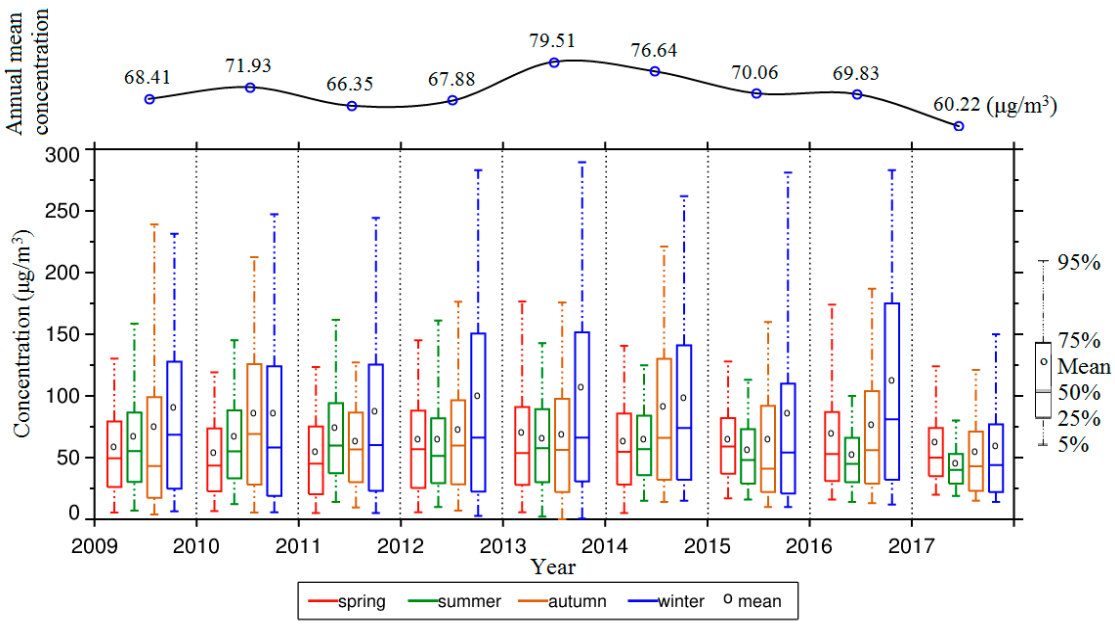

Figure 2. Seasonal and annual variations of particulate matter with an aerodynamic diameter less than or equal to 2.50 μm ($PM_{2.5}$) concentrations. The circles show seasonal mean values together with the 95th, 75th, 50th, 25th, and 5th percentiles. The numbers on the top of the figures represent the annual mean values.

3.2. Transport Pathways

Six clusters were produced by the clustering algorithm for Tianjin from March 2009 to February 2018, and the cluster-mean back trajectories and their air pressure profiles are shown in Figures 3 and 4. Distributions of $PM_{2.5}$ concentrations associated with six trajectory clusters on a seasonal basis are presented in Figure 5. The velocity of air mass movement could be judged according to the length of the trajectory. Long trajectories corresponded to fast-moving air masses, while short trajectories corresponded to slow-moving air masses. According to the mean $PM_{2.5}$ mass concentration of Tianjin corresponding to each cluster, the cluster-mean backward trajectories were divided into clean pathways and pollution pathways. A cluster-mean backward trajectory corresponding to a $PM_{2.5}$ concentration in Tianjin > 75.00 μg/m^3 was defined as a pollution pathway. On the contrary, a cluster-mean backward trajectory corresponding to a $PM_{2.5}$ concentration in Tianjin < 75.00 μg/m^3 was defined as a clean pathway. A cluster-mean back trajectory was also defined as a pollution pathway if the amount of pollution trajectories in this cluster accounted for more than one-sixth of the total number of pollution trajectories.

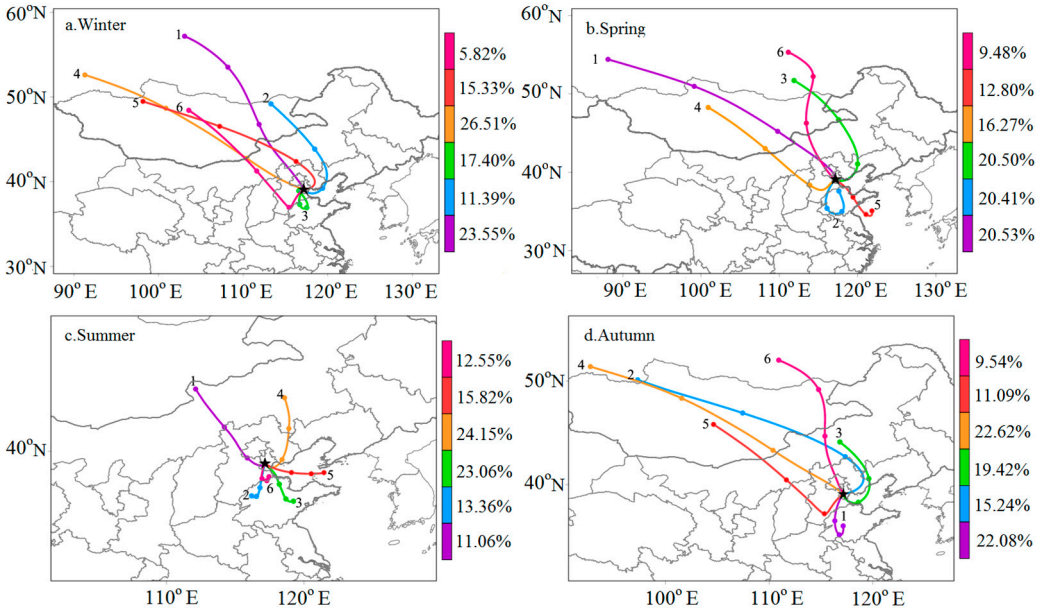

Figure 3. Cluster-mean back trajectories of (**a**) winter, (**b**) spring, (**c**) summer and (**d**) autumn from 2009 to 2018. The dots on the trajectories represent time nodes (24 h, 48 h, 72 h). The percentage represents the ratio of the number of back trajectories in each cluster to the total number of back trajectories. The black star represents Tianjin.

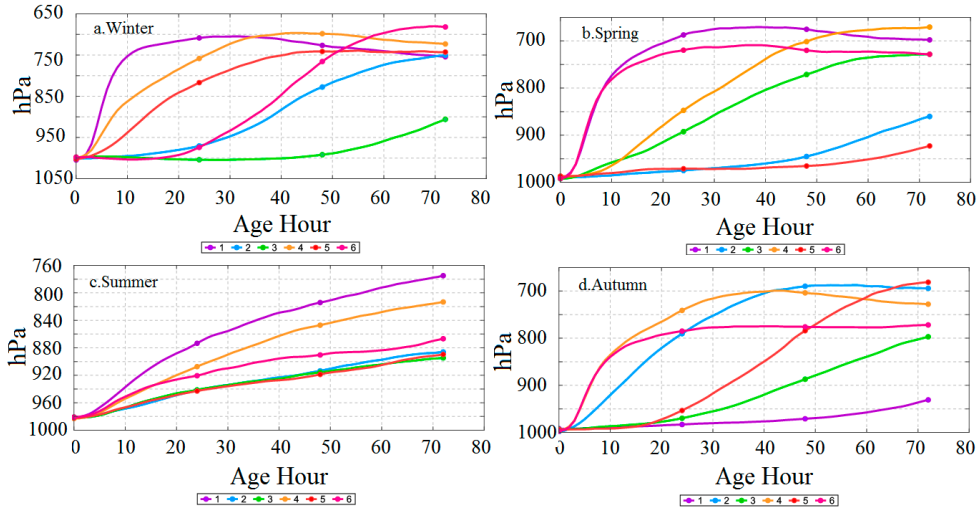

Figure 4. Air pressure profiles of the backward trajectories in (**a**) winter, (**b**) spring, (**c**) summer and (**d**) autumn.

In winter, it was found that four out of the six cluster trajectories, represented by clusters 3, 4, 5, and 6, were pollution pathways. Among these four major pathways, the one shown as cluster 3 accounted for 17.40% and was the most polluted. More than 85% of its sample concentrations exceeded the daily class II standard of $PM_{2.5}$, and the mean concentration (168.00 μg/m^3) was far above the daily standard concentration (Figure 5). Cluster 3 originated from Hebei, went through Shandong, and reached Tianjin. This was a regional transport pathway within a boundary layer (Figure 4a). Its short length suggested low wind velocity. Low wind velocity and relatively low boundary layer heights in winter may exacerbate air pollution, contributing to a severe haze episode. The second most polluted pathway was cluster 6, which meant the concentration was 120.00 μg/m^3. More than 75% of the sample concentrations exceeded daily class II standard concentrations (Figure 5). The air masses associated

with cluster 6 were from Central Mongolia, moved southeasterly over the Inner Mongolian Plateau and into Hebei, and finally turned northeast to Tianjin. The air masses of cluster 6 from the southwest were transported in the boundary layer and slowed down in the first 24 h. Cluster 4, which meant the concentration was 92.00 μg/m^3, was the prevalent trajectory pathway in winter (26.51%). The air masses associated with both clusters 4 and 5 initially traveled southeasterly over desert and semidesert regions of Mongolia and the Hunshandake sand lands of Inner Mongolia. Cluster 4 air masses then went southeasterly though Hebei and Beijing to Tianjin. Cluster 5 finally turned northwest though Hebei to Tianjin. Clusters 4, 5, and 6 all passed though Mongolia and Inner Mongolia: A study by Zhao et al. [42] showed that long-range transport from Inner Mongolia also had an adverse effect on $PM_{2.5}$ in Shanghai. Clusters 1 and 2 were clean pathways for Tianjin in winter. The air masses associated with clusters 1 and 2 originated from Lake Baikal and Outer Mongolia. Cluster 1 air masses moved rapidly and traveled at heights greater than 750 hPa for the 10 h before arrival in Tianjin. Cluster 2 represented a relatively slow-moving air mass, particularly in the 24 h preceding its arrival in Tianjin. It reached Tianjin through the Bay of Bohai and was considered to be a relatively clean trajectory. It can be seen from Table 1 that the highest percentage of polluted trajectories (37.70%) and the highest $PM_{2.5}$ loading (182.00 μg/m^3) were observed in cluster 3, followed by clusters 4 and 6. In addition, 89.60% of total trajectories in cluster 3 were polluted trajectories, and 25.00% and 10.70% of total polluted trajectories were from the cluster 4 and cluster 6 trajectories, respectively: 77.60% of the trajectories in cluster 6 were polluted.

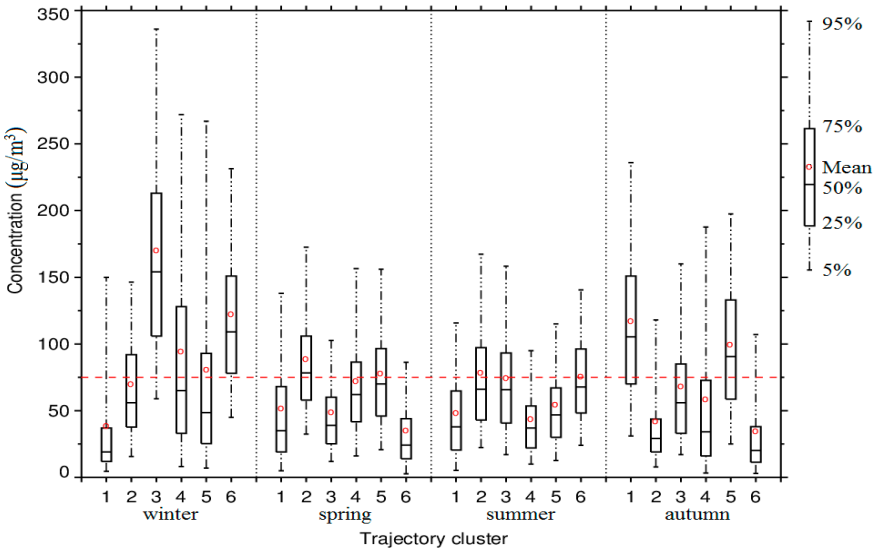

Figure 5. Box plots of $PM_{2.5}$ concentrations associated with six trajectory clusters on a seasonal basis. The red circles indicate the arithmetic mean. The red dashed lines represent the Chinese national class II standard of $PM_{2.5}$ daily mean concentrations.

In spring, the pollution pathways associated with trajectory clusters 2, 4, and 5 accounted for 20.41%, 16.27%, and 12.80% (Figure 3). Cluster 2 was the major pollution pathway, followed by clusters 4 and 5. The mean concentrations of clusters 2, 4, and 5 were 87.00 μg/m^3, 70.00 μg/m^3, and 76.00 μg/m^3 (Figure 5). Clusters 2 and 5 were both short pathways and were transported into the boundary layer. Cluster 2 air masses were from Northern Shandong and traveled southerly, finally going northerly through Shandong to Tianjin. Cluster 5 air masses originated from the Bohai Sea and then traveled northwesterly through Shandong to Tianjin. Thus, the pathways through Shandong were noticeable for Tianjin in the spring. Cluster 4 was from Central Mongolia, moving southeasterly over Inner Mongolia, Shanxi, and Hebei and finally turning northeasterly to Tianjin. The air masses of cluster 4 were transported below 925 hPa and slowed down in the first 20 h before reaching Tianjin

(Figure 4b). The one shown as cluster 2 had the largest percentage (37.90%) of polluted trajectories and a higher mean loading (114.00 μg/m^3) (Table 1). More than half of the trajectories in cluster 2 were pollution trajectories. Although the mean concentration of cluster 4 in spring did not exceed the class II standard concentration, the pollution trajectories in cluster 4 accounted for 18.10% of the total pollution trajectories. Cluster 5 contributed 17.00% of the total pollution trajectories.

Table 1. Trajectory percentage and mean $PM_{2.5}$ concentrations based on all trajectories and pollution trajectories.

Season	Cluster	Number of All Trajectories per Cluster	Percentage of Pollution Trajectories in Each Cluster (%)	Percentage of Pollution Trajectories in Total Pollution Trajectories Per Season (%)	Mean Concentration and Standard Deviation of Pollution Trajectories (μg/m^3)
Winter	1	620	12.10	6.40	147 ± 74
	2	323	34.40	9.50	116 ± 43
	3	490	89.60	37.70	182 ± 82
	4	690	42.20	25.00	167 ± 91
	5	393	31.30	10.60	176 ± 109
	6	161	77.60	10.70	140 ± 53
Spring	1	553	21.90	14.40	117 ± 44
	2	574	55.40	37.90	114 ± 37
	3	588	14.30	10.00	106 ± 33
	4	454	33.50	18.10	116 ± 48
	5	325	44.00	17.00	112 ± 33
	6	250	8.40	2.50	107 ± 46
Summer	1	324	18.20	6.90	108 ± 27
	2	395	42.80	19.70	117 ± 38
	3	717	40.00	33.40	114 ± 35
	4	714	10.90	9.10	99 ± 21
	5	499	19.40	11.30	107 ± 40
	6	388	43.30	19.60	108 ± 30
Autumn	1	588	71.40	42.40	142 ± 57
	2	377	9.30	3.50	144 ± 73
	3	538	32.00	17.40	119 ± 40
	4	593	24.30	14.50	144 ± 73
	5	320	60.10	19.70	129 ± 42
	6	226	10.60	2.40	117 ± 37

In summer, the higher levels of $PM_{2.5}$ concentration in Tianjin coincided with trajectories grouped in clusters 2, 3, and 6, which were all southerly short pathways and accounted for 48.97% of the total number of trajectories (Figure 3). The mean concentrations of clusters 2, 3, and 6 were 77.00 μg/m^3, 72.00 μg/m^3, and 74.00 μg/m^3. Cluster 2 and cluster 3 originated from northwestern and eastern Shandong, respectively, and traveled north in the 24 h preceding their arrival in Tianjin. Cluster 6 originated from Hebei and traveled south to Shandong and then north to Tianjin. The transport heights of pollution pathways were all less than 850 hPa (Figure 4c). Cluster 3 had the largest percentage (33.40%) of polluted trajectories, and the pollution pathways accounted for 40.00% of all pathways for cluster 3 (Table 1).

In autumn, clusters 1, 3, and 5 were the pollution pathways, the mean concentrations of which were 115.00 μg/m^3, 66.00 μg/m^3, and 98.00 μg/m^3. Cluster 1 originated from Shandong and went northerly to Tianjin, the transport height of which was less than 925 hPa (Figure 4d). Cluster 3 originated from Inner Mongolia and passed over the Bohai Sea and Shandong before reaching Tianjin. This was the only pollution pathway through the sea. However, in the 24 h preceding its arrival in Tianjin, the air masses of cluster 3 arrived in Shandong and moved slowly, the heights of which were below 925 hPa. Cluster 5 in autumn, similarly to cluster 6 in winter, was from Central Mongolia, moved southeasterly over the Inner Mongolian Plateau and into Hebei, and finally turned northeasterly to Tianjin. The air masses of cluster 5 from the southwest direction were transported below 925 hPa and slowed down in the 24 h preceding their arrival in Tianjin. The highest probability (71.40%) of pollution trajectories occurred in cluster 1, which contributed 42.00% of polluted trajectories (Table 1).

The mean loading of polluted trajectories in cluster 1 was 142.00 μg/m^3, 60.10% of the trajectories in cluster 5 were pollution trajectories, and 19.70% and 17.40% of pollution trajectories came from cluster 5 and cluster 3, respectively.

3.3. Wind Dependence of $PM_{2.5}$ Loadings

The seasonal wind roses with $PM_{2.5}$ loadings on the west coast of Bohai Bay using hourly data for 2009–2018 are shown in Figure 6. The prevailing winds for winter were between the north and the northwest. Most of winds were abundant, with the south and southeast as the prevailing wind directions in summer. The variation in wind direction in different seasons is because this area is located in a monsoon zone, with prevailing winds from northern directions during winter and from southern directions during summer. Winds from the northwest and north originate from or pass over economically underdeveloped regions in China with relatively lower $PM_{2.5}$ emissions intensities.

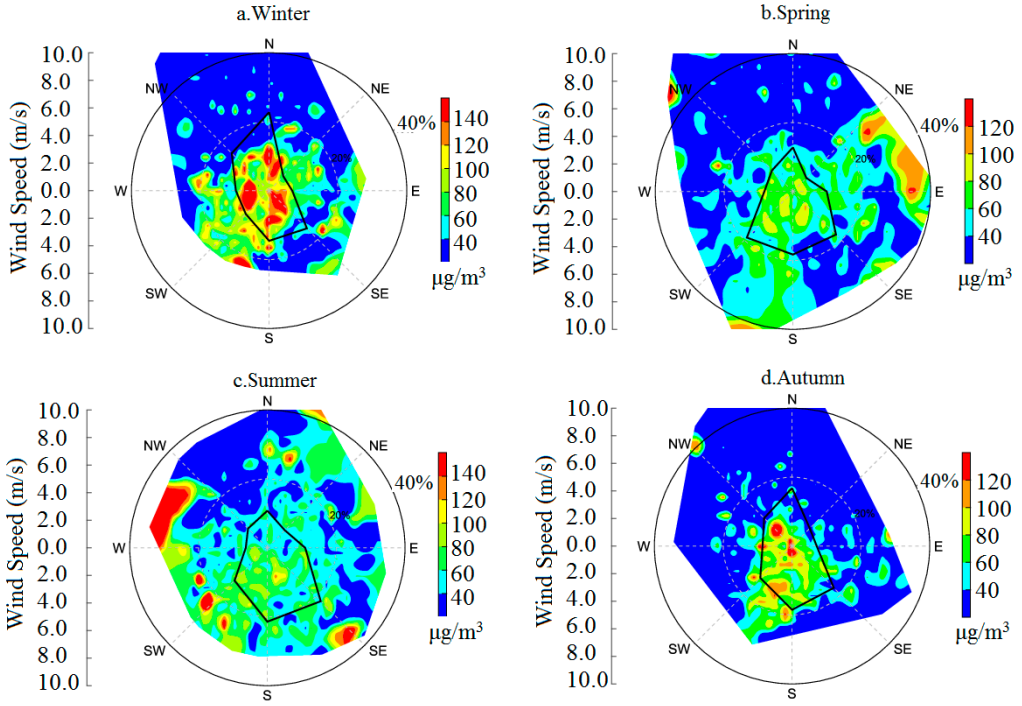

Figure 6. Wind roses with $PM_{2.5}$ concentrations in (**a**) winter, (**b**) spring, (**c**) summer and (**d**) autumn durng 2009–2018.

$PM_{2.5}$ loadings showed pronounced dependence on the wind, especially in the heavily polluted autumn and winter. As shown in Figure 6a, high $PM_{2.5}$ concentrations were mainly concentrated in low wind speed (0–2 m/s) areas and were associated with winds from the south and west. Southern winds and western winds were normally from the Shanxi, Shandong, and Hebei provinces. Regardless of the wind directions, $PM_{2.5}$ loadings were below 40.00 μg/m^3 when the wind speeds were greater than 6 m/s. Most of the high $PM_{2.5}$ loadings in autumn were associated with winds from the south and southwest, and wind speeds were all in the range of 0–5 m/s. The situation in spring and summer showed a similar but less pronounced directional dependence compared to winter and autumn. High $PM_{2.5}$ loadings were observed with northeasterly to easterly flows in spring (Figure 6b) and northwesterly to westerly flows in summer (Figure 6c). Overall, the southwesterly winds had an adverse effect on $PM_{2.5}$ loadings in different seasons for Tianjin. In contrast, wind from the northwest to north sectors normally showed mean $PM_{2.5}$ loadings lower than 40.00 μg/m^3.

3.4. Potential Source Regions

The PSCF maps covering the study period that are shown in Figure 7 were plotted in order to identify the probable locations of potential source regions contributing to $PM_{2.5}$ levels in Tianjin on the west coast of Bohai Bay. In general, the main source areas were all in the south of Tianjin. The potential source areas for winter were larger than for other seasons. In winter, the major source areas of $PM_{2.5}$, with WPSCF values of 0.80–1.00, were in the junction of Hebei, Henan, and Shandong. Northern Shandong, southern Hebei, northeastern Henan, northern Shanxi, central Inner Mongolia, and northern Mongolia were also potential source areas of $PM_{2.5}$, with WPSCF values of 0.50–0.80. This was mainly because these areas, except for Inner Mongolia and Mongolia, are economically developed industrial areas, and pathways of air masses ended at Tianjin. The Gobi Desert in central Inner Mongolia and northern Mongolia was a natural source of $PM_{2.5}$. In autumn, the major potential sources were located in eastern Henan, northwestern Shandong, and northern Hebei (Figure 7d). North central Hebei, central Shandong, Shanxi, northern Jiangsu, and northern Anhui were the second potential source areas. The domains of major sources in winter and autumn were all concentrated in the southwest of Tianjin, which revealed that transport from the southwest was more important for heavy $PM_{2.5}$ pollution in winter and autumn. The potential source regions determined from the PSCF analysis coincided with the results from the wind dependence of $PM_{2.5}$ loadings. However, the major potential source areas varied seasonally. In spring, major sources of $PM_{2.5}$, with WPSCF values of 0.50–0.70, were in Shandong, eastern Henan, and northern Anhui and Jiangsu, and for summer were in northern Jiangsu and western Shandong.

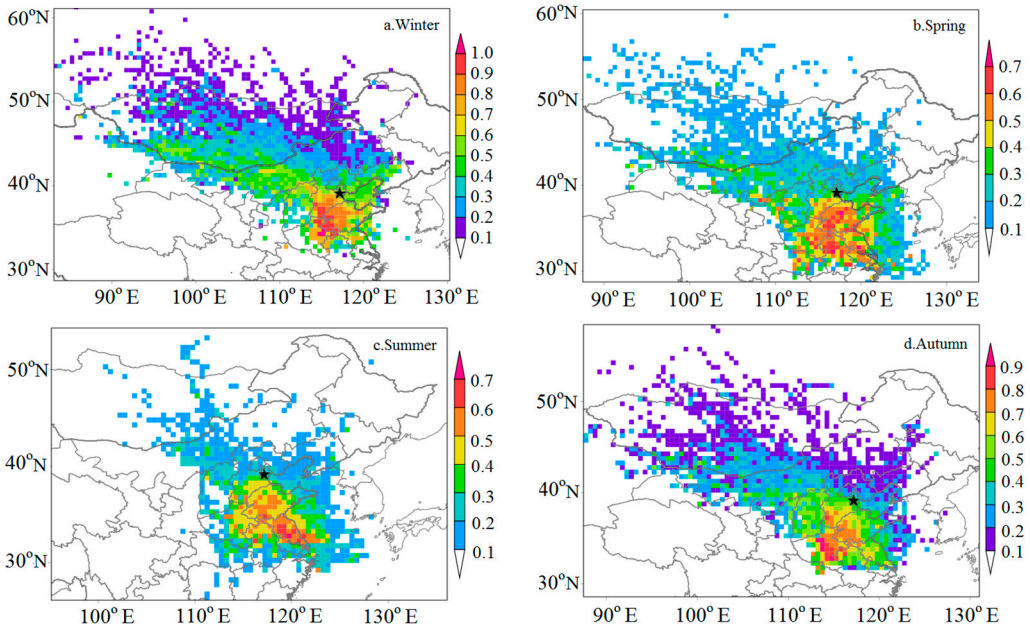

Figure 7. Weighted potential source contribution function (PSCF) maps of $PM_{2.5}$ in (**a**) winter, (**b**) spring, (**c**) summer and (**d**) autumn during 2009–2018. The black star represents Tianjin.

Since the PSCF method can only reflect the contribution rate of the potential source regions, that is, the proportion of pollution trajectories in each grid, it cannot reflect the pollution degree of the potential source regions. In order to study the contribution of pollutants in potential source regions, the CWT method was used to reflect the pollution degree of different trajectories. The results for $PM_{2.5}$ loadings identified through the CWT method in Figure 8 were somewhat different from the results analyzed through the PSCF method. WCWT values do not represent the regions' actual contributions. Instead, they demonstrate the relative importance of the source regions [31]. In winter, the highest WCWT values covering the map were distributed in southern Hebei, western Shandong,

and northeastern Anhui. Those areas were the main contribution sources associated with the highest $PM_{2.5}$ loadings (exceeding 140.00 μg/m^3), and the border between Anhui and Shandong was even higher than 200.00 μg/m^3. This demonstrated that contributions of transportation and source regions from southern Tianjin were significant. As shown in Figure 8a, there were also secondary source areas in winter, namely central Inner Mongolia and southern Mongolia. These areas are normally characterized by land forms of sand and the Gobi Desert. Besides the impact of local and regional potential sources, long-range transport also played some role in $PM_{2.5}$ loadings in winter. This depended on both the prevailing northwest wind in Tianjin and potential source areas to the northwest, contributing to the long-rang transport of $PM_{2.5}$. In spring and summer, the maximum WCWT was much smaller than in winter. The significant potential source regions in spring were identified south of Tianjin, including southern Hebei, Shandong, eastern Henan, northern Anhui, and Jiangsu. In addition to the above areas, a small part of the Yellow Sea was also included in the summer (adjacent to Jiangsu province). In autumn, the highest WCWT values (exceeding 100.00 μg/m^3) were mainly located in southern Hebei, western Shandong, eastern Henan, the northwest corner of Anhui, and parts of Jiangsu. The second potential source areas were Shanxi, central Shandong, and northern Jiangsu.

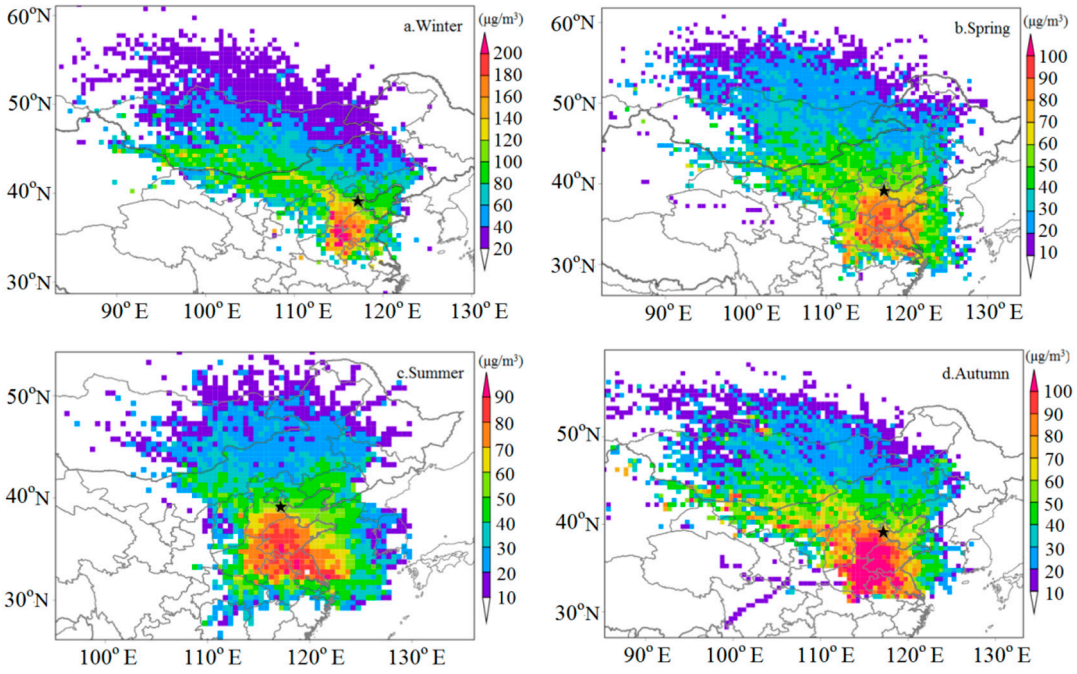

Figure 8. Weighted concentration weighted trajectory (CWT) map of $PM_{2.5}$ in (**a**) winter, (**b**) spring, (**c**) summer and (**d**) autumn during 2009–2018. The black star represents Tianjin.

The PSCF and CWT analyses gave similar potential source locations, but the contributions of these locations were different. The major potential source areas derived from the CWT method were larger than those of the PSCF method, especially in autumn and summer. Regional sources might play a more pronounced role in the distribution of $PM_{2.5}$ in Tianjin. The most possible major source regions of $PM_{2.5}$ were located within about 800 km south of Tianjin, and no significant long-range transport processes contributed to $PM_{2.5}$ loadings in Tianjin except for in winter and autumn.

3.5. Comparison to Anthropogenic Emissions Inventory

The spatially disaggregated Chinese anthropogenic emissions inventory for $PM_{2.5}$ in 2016 is shown in Figure 9. Most of the $PM_{2.5}$ emission sources were concentrated in the Beijing–Tianjin–Hebei region and its surrounding areas, including Beijing, Tianjin, Hebei, Shandong, Shanxi, and Henan (see Figure 9). Beijing–Tianjin–Hebei and its surrounding areas are urbanized and industrialized

regions with high anthropogenic $PM_{2.5}$ emissions. In North China, there are densely populated regions, numerous metallurgical works, and coal-related industries. Other regions with high concentrations of emissions sources are the Yangtze River Delta, which includes Shanghai, Jiangsu, and Zhejiang, and some parts of the southwest.

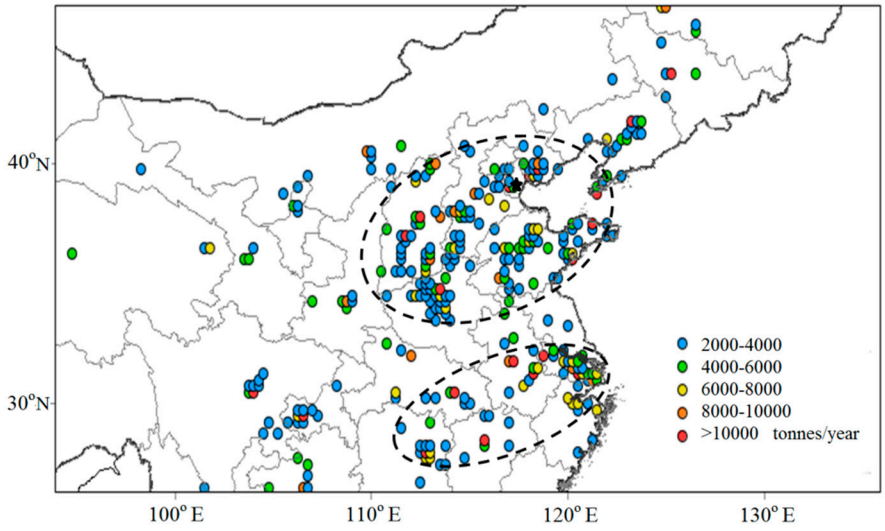

Figure 9. Spatial distributions of anthropogenic emissions of $PM_{2.5}$ for China in 2016. The black star represents Tianjin.

According to the above research, the potential sources of Tianjin were mainly composed of two regions (Figure 10). The major sources were the south of Tianjin, including southern Hebei, western Shandong, eastern Henan, northern Anhui, and northern Jiangsu. The secondary sources, which were northwesterly sources, encompassed central Inner Mongolia and southern Mongolia. The potential source regions determined from the PSCF and CWT analyses coincided with the emissions of $PM_{2.5}$ in North China and the results from the wind dependence of $PM_{2.5}$ loadings. Based on the above results, we preliminarily considered that the major source areas were anthropogenic sources and the secondary source areas were natural sources. This conclusion was consistent with the fact that dust aerosols are transported to Beijing from northwestern regions in spring [43,44], and anthropogenic aerosols are transported from the south [45,46]. The pathways were classified into two broad categories according to the distribution of directions of pollution clusters in Tianjin. Thus, the southerly pathway and northwesterly pathway were two major transport channels contributing to high $PM_{2.5}$ concentrations in Tianjin. The southerly transport pathway from major sources, namely the regional transport pathway, played an important role in $PM_{2.5}$ concentrations in all seasons in Tianjin. It had the greatest impact on $PM_{2.5}$ levels registered during winter, followed by autumn, and had the least impact in summer. Air masses originating from major sources probably were transported within the boundary layer and moved slowly to Tianjin. The northwesterly transport pathway from secondary sources, namely the long-range transport pathway, affected $PM_{2.5}$ concentrations in the winter, autumn, and spring. This conclusion was different from that reached by Liang et al. [20] in Beijing, where a long-rang transport from the northwest was identified as the prevailing $PM_{2.5}$ pollution transport in spring and in summer. The influence of the northwesterly pathway on $PM_{2.5}$ concentrations in Tianjin was also less than that of the southerly pathway.

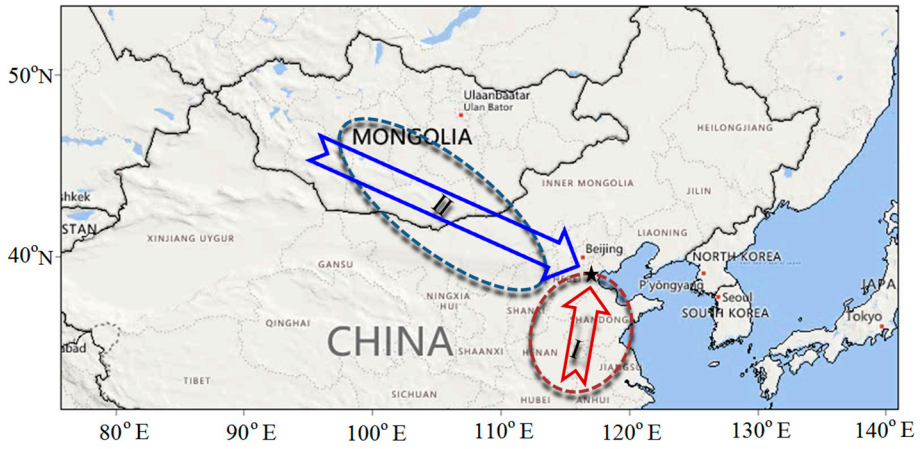

Figure 10. Schematic diagram of transport pathways and potential sources of $PM_{2.5}$ (red arrow: Transport pathway in all seasons; blue arrow: Transport pathway only in winter, autumn, and spring; I: Major source; II: Secondary source).

4. Conclusions

Transport pathways and potential source regions of $PM_{2.5}$ on the west coast of Bohai Bay were identified through cluster trajectory, PSCF, and CWT methods based on 2009–2018 data. The annual $PM_{2.5}$ levels varied between 68.41 and 67.88 μg/m^3 from 2009 to 2012, reaching their maximum value (79.51 μg/m^3) in 2013 and then declining steadily ever since. High $PM_{2.5}$ concentrations always occurred in the winter, followed by autumn and spring.

Two transport pathways of high $PM_{2.5}$ concentrations in the west coast of Bohai Bay (in the broad sense) were identified, namely a southerly pathway and a northwesterly pathway. The southerly pathway represented the major transport pathway of $PM_{2.5}$ for all seasons. It had the greatest impact in winter, followed by autumn. The air masses associated with the southerly pathway were transported within the boundary layer (below 925 hPa) and moved slowly to Tianjin. The southerly transport pathway passed over the Shandong and Hebei provinces before reaching Tianjin. The northwesterly pathway belonging to long-range transport mainly affected $PM_{2.5}$ concentrations in winter and moved faster. The northwesterly pathways passed over desert and semidesert regions in Outer Mongolia, the sand lands of Inner Mongolia, and Hebei.

The potential source regions contributing to high $PM_{2.5}$ loadings on the west coast of Bohai Bay could be grouped into two broad categories, the "southerly source regions" (southern Hebei, western Shandong, eastern Henan, northern Anhui, and northern Jiangsu) and the "northwesterly source regions" (central Inner Mongolia and southern Mongolia). The "southerly source regions" were decided upon after a comparison to the Chinese spatially disaggregated anthropogenic emissions inventory and were identified as anthropogenic source regions, while the "northwesterly source regions" were regarded as natural source regions. Moreover, the major transport pathway passed over anthropogenic source regions, while the secondary transport pathway passed though natural source regions. The impacts of anthropogenic source regions on $PM_{2.5}$ loadings on the west coast of Bohai Bay were much greater than those of natural source regions. However, additional studies on the secondary reaction of $PM_{2.5}$ on the west coast of Bohai Bay are warranted to elucidate the variability in potential source regions of $PM_{2.5}$.

It can be seen from the above results that adjacent source regions had a relatively great impact on $PM_{2.5}$ concentrations on the west coast of Bohai Bay. Therefore, the meteorological characteristics of each pollution pathway, such as temperature, and the specific contribution of the adjacent source regions need to be studied further in detail.

Author Contributions: Conceptualization, S.H. and T.H.; Methodology, T.H.; Software, T.H.; Validation, Q.Y. and W.F.; Formal analysis, Z.C.; Data curation, Z.C. and Q.Y.; Writing—original draft preparation, T.H. and Z.C.; Writing—review and editing, T.H. and W.F.; Supervision, S.H.; Project administration, S.H.; Funding acquisition, S.H.

Funding: This research was funded by the National Science and the National Major Projects (2016YFC0203302), the National Natural Science Foundation of China (41771242), the Natural Science Foundation of Tianjin (18JCYBJC23100), the science and technology support program of the ministry of science and technology of China (2014BAC16B04), and the scientific research project of Tianjin Meteorological Bureau (201736bsjj02).

Acknowledgments: We express our gratitude to Yaqiang Wang (Center for Atmosphere Watch and Services, Chinese Academy of Meteorological Sciences) who provided guidance on the proper use of software.

Conflicts of Interest: The authors declare no conflict of interest.

References

1. Chan, C.; Yao, X. Air pollution in mega cities in China. *Atmos. Environ.* **2008**, *42*, 1–42. [CrossRef]
2. Shao, M.; Tang, X.; Zhang, Y.; Li, W. City clusters in China: Air and surface water pollution. *Front. Ecol. Environ.* **2006**, *4*, 353–361. [CrossRef]
3. Zhao, P.; Zhang, X. Long-term visibility trends and characteristics in the region of Beijing, Tianjin, and Hebei, China. *Atmos. Res.* **2011**, *101*, 711–718. [CrossRef]
4. Fang, M.; Chan, C.K.; Yao, X. Managing air quality in a rapidly developing nation: China. *Atmos. Environ.* **2009**, *43*, 79–86. [CrossRef]
5. Zhang, M.; Song, Y.; Cai, X. A health-based assessment of particulate air pollution in urban areas of Beijing in 2000–2004. *Sci. Total Environ.* **2007**, *376*, 100–108. [CrossRef] [PubMed]
6. Alolayan, M.A.; Brown, K.W.; Evans, J.S.; Bouhamra, W.S.; Koutrakis, P. Source apportionment of fine particles in kuwait city. *Sci. Total Environ.* **2013**, *448*, 14–25. [CrossRef] [PubMed]
7. Hellack, B.; Quass, U.; Beuck, H.; Wick, G.; Kuttler, W.; Schins, R.P.; Kuhlbusch, T.A. Elemental composition and radical formation potency of PM_{10} at an urban background station in Germany in relation to origin of air masses. *Atmos. Environ.* **2015**, *105*, 1–6. [CrossRef]
8. Makra, L.; Ionel, I.; Csépe, Z.; Matyasovszky, I.; Lontis, N.; Popescu, F.; Sümeghy, Z. The effect of different transport modes on urban PM10 levels in two European cities. *Sci. Total Environ.* **2013**, *458*, 36–46. [CrossRef]
9. Kong, X.; He, W.; Qin, N.; He, Q.; Yang, B.; Ouyang, H.; Wang, Q.; Xu, F. Comparison of transport pathways and potential sources of PM10 in two cities around a large Chinese lake using the modified trajectory analysis. *Atmos. Res.* **2013**, *122*, 284–297. [CrossRef]
10. Zhang, R.; Jing, J.; Tao, J.; Hsu, S.C. Chemical characterization and source apportionment of $PM_{2.5}$ in Beijing: Seasonal perspective. *Atmos. Chem. Phys.* **2014**, *13*, 7053–7074. [CrossRef]
11. Lai, L.W. Fine particulate matter events associated with synoptic weather patterns, long-range transport paths and mixing height in the Taipei basin, Taiwan. *Atmos. Environ.* **2015**, *113*, 50–62. [CrossRef]
12. Lv, B.; Zhang, B.; Bai, Y. A systematic analysis of $PM_{2.5}$ in Beijing and its sources from 2000 to 2012. *Atmos. Environ.* **2016**, *124*, 98–108. [CrossRef]
13. Fuelberg, H.E.; Kiley, C.M.; Hannan, J.R.; Westberg, D.J.; Avery, M.A.; Newell, R.E. Meteorological conditions and transport pathways during the transport and chemical evolution over the pacific (trace-p) experiment. *J. Geophys. Res. Atmos.* **2003**, *108*, 8782. [CrossRef]
14. Reid, J.S.; Lagrosas, N.D.; Jonsson, H.H.; Reid, E.A.; Atwood, S.A.; Boyd, T.J.; Ghate, V.P.; Xian, P.; Posselt, D.J.; Simpas, J.B.; et al. Aerosol meteorology of Maritime Continent for the 2012 7SEAS southwest monsoon intensive study–Part 2: Philippine receptor observations of fine-scale aerosol behavior. *Atmos. Chem. Phys.* **2016**, *16*, 14057–14078. [CrossRef]
15. He, K.; Huo, H.; Zhang, Q. Urban air pollution in China: Current status, characteristics, and progress. *Annu. Rev. Energy Environ.* **2011**, *27*, 397–431. [CrossRef]
16. Wang, G.C.; Wang, J.; Xin, Y.J.; Chen, L. Transportation pathways and potential source areas of PM_{10} and NO_2 in Tianjin. *China. Environ. Sci* **2014**, *34*, 3009–3016. (In Chinese)
17. Wang, Y.Q.; Zhang, X.Y.; Arimoto, R. The contribution from distant dust sources to the atmospheric particulate matter loadings at XiAn, China during spring. *Sci. Total Environ.* **2006**, *368*, 875–883. [CrossRef] [PubMed]

18. Xin, Y.J.; Wang, G.C.; Chen, L. Identification of long-range transport pathways and potential sources of PM_{10} in Tibetan Plateau uplift area: Case study of Xining, China in 2014. *Aerosol Air Qual. Res.* **2016**, *16*, 1044–1054. [CrossRef]
19. Zhu, L.; Huang, X.; Shi, H.; Cai, X.; Song, Y. Transport pathways and potential sources of PM_{10} in Beijing. *Atmos. Environ.* **2011**, *45*, 594–604. [CrossRef]
20. Liang, D.; Wang, Y.Q.; Ma, C.; Wang, Y.J. Variability in transport pathways and source areas of PM_{10} in Beijing during 2009–2012. *Aerosol Air Qual. Res.* **2016**, *16*, 3130–3141. [CrossRef]
21. Wang, L.; Liu, Z.; Sun, Y.; Ji, D.; Wang, Y. Long-range transport and regional sources of $PM_{2.5}$ in Beijing based on long-term observations from 2005 to 2010. *Atmos. Res.* **2015**, *157*, 37–48. [CrossRef]
22. Ashbaugh, L. A statistical trajectory technique for determining air pollution source regions. *J. Air Pollut. Control Assoc.* **1983**, *33*, 1096–1098. [CrossRef]
23. Sirois, A.; Bottenheim, J.W. Use of backward trajectories to interpret the 5-year record of PAN and O_3 ambient air concentrations at Kejimkujik National Park, Nova Scotia. *J. Geophys. Res. Atmos.* **1995**, *100*, 2867–2881. [CrossRef]
24. Park, S.S.; Lee, K.H.; Kim, Y.J.; Kim, T.Y.; Cho, S.Y.; Kim, S.J. High time-resolution measurements of carbonaceous species in $PM_{2.5}$ at an urban site of Korea. *Atmos. Res.* **2008**, *89*, 48–61. [CrossRef]
25. Moody, J.L.; Galloway, J.N. Quantifying the relationship between atmospheric transport and the chemical composition of precipitation on Bermuda. *Tellus B* **1988**, *40*, 463–479. [CrossRef]
26. Harris, J.M.; Kahl, J.D. A descriptive atmospheric transport climatology for the Mauna Loa Observatory, using clustered trajectories. *J. Geophys. Res. Atmos.* **1990**, *95*, 13651–13667. [CrossRef]
27. Dorling, S.R.; Davies, T.D.; Pierce, C.E. Cluster analysis: A technique for estimating the synoptic meteorological controls on air and precipitation chemistry-method and applications. *Atmos. Environ.* **1992**, *26*, 2575–2581. [CrossRef]
28. Vasconcelos, L.A.D.P.; Kahl, J.D.W.; Liu, D.; Macias, E.S.; White, W.H. Spatial resolution of a transport inversion technique. *J. Geophys. Res. Atmos.* **1996**, *101*, 19337–19342. [CrossRef]
29. Seibert, P.; Kromp-Kolb, H.; Baltensperger, U.; Jost, D.T.; Schwikowski, M.; Kasper, A.; Puxbaum, H. Trajectory analysis of aerosol measurements at high alpine sites. In *Transport and Transformation of Pollutants in the Troposphere*; Borrel, P.M., Borrel, P., Cvitas, T., Seiler, W., Eds.; Academic Publishing: Den Haag, The Netherlands, 1994; pp. 689–693.
30. Stohl, A. Trajectory statistics-a new method to establish source-receptor relationships of air pollutants and its application to the transport of particulate sulfate in Europe. *Atmos. Environ.* **1996**, *30*, 579–587. [CrossRef]
31. Hsu, Y.K.; Holsen, T.M.; Hopke, P.K. Comparison of hybrid receptor models to locate PCB sources in Chicago. *Atmos. Environ.* **2003**, *37*, 545–562. [CrossRef]
32. Sun, Y.; Song, T.; Tang, G.; Wang, Y. The vertical distribution of PM2.5 and boundary-layer structure during summer haze in Beijing. *Atmos. Environ.* **2013**, *74*, 413–421. [CrossRef]
33. Wang, Y.Q.; Zhang, X.Y.; Draxler, R.R. Trajstat: Gis-based software that uses various trajectory statistical analysis methods to identify potential sources from long-term air pollution measurement data. *Environ. Modell. Softw.* **2009**, *24*, 938–939. [CrossRef]
34. Environmental Protection Department, State Administration of Quality Supervision, Inspection and Quarantine. Ambient Air Quality Standards. In *The State Standard of the People's Republic of China GB*; Environmental Science Press: Beijing, China, 2012. (In Chinese)
35. Zeng, Y.; Hopke, P.K. A study of the sources of acid precipitation in Ontario, Canada. *Atmos. Environ.* **1989**, *23*, 1499–1509. [CrossRef]
36. Polissar, A.V.; Hopke, P.K.; Paatero, P.; Kaufmann, Y.J.; Hall, D.K.; Bodhaine, B.A.; Dutton, E.G.; Harris, J.M. The aerosol at Barrow, Alaska: Long-term trends and source locations. *Atmos. Environ.* **1999**, *33*, 2441–2458. [CrossRef]
37. Begum, B.A.; Kim, E.; Jeong, C.H.; Lee, D.W.; Hopke, P.K. Evaluation of the potential source contribution function using the 2002 Quebec forest fire episode. *Atmos. Environ.* **2005**, *39*, 3719–3724. [CrossRef]
38. Polissar, A.V.; Hopke, P.K.; Harris, J.M. Source regions for atmospheric aerosol measured at Barrow, Alaska. *Environ. Sci. Technol.* **2001**, *35*, 4214–4226. [CrossRef] [PubMed]
39. Polissar, A.V.; Hopke, P.K.; Poirot, R.L. Atmospheric aerosol over Vermont: Chemical composition and sources. *Environ. Sci. Technol.* **2001**, *35*, 4604–4621. [CrossRef]

40. Karaca, F.; Anil, I.; Alagha, O. Long-range potential source contributions of episodic aerosol events to PM profile of a megacity. *Atmos. Environ.* **2009**, *43*, 5713–5722. [CrossRef]
41. Xu, X.; Akhtar, U.S. Identification of potential regional sources of atmospheric total gaseous mercury in windsor, Ontario, Canada using hybrid receptor modeling. *Atmos. Chem. Phys.* **2010**, *10*, 7073–7083. [CrossRef]
42. Zhao, M.; Huang, Z.; Qiao, T.; Zhang, Y.; Xiu, G.; Yu, J. Chemical characterization, the transport pathways and potential sources of PM2.5, in Shanghai: Seasonal variations. *Atmos. Res.* **2015**, *158*, 66–78. [CrossRef]
43. Wang, Y.Q.; Zhang, X.Y.; Arimoto, R.; Cao, J.J.; Shen, Z.X. The transport pathways and sources of PM10 pollution in Beijing during spring 2001, 2002 and 2003. *Geophys. Res. Lett.* **2004**, *31*, 14. [CrossRef]
44. Zhao, X.; Zhuang, G.; Wang, Z.; Sun, Y.; Wang, Y.; Yuan, H. Variation of sources and mixing mechanism of mineral dust with pollution aerosol-revealed by the two peaks of a super dust storm in Beijing. *Atmos. Res.* **2007**, *84*, 265–279. [CrossRef]
45. Xia, X.; Chen, H.; Zhang, W. Analysis of the dependence of column-integrated aerosol properties on long-range transport of air masses in Beijing. *Atmos. Environ.* **2007**, *41*, 7739–7750. [CrossRef]
46. Wehner, B.; Birmili, W.; Ditas, F.; Wu, Z.; Hu, M.; Liu, X.; Mao, J.; Sugimoto, N.; Wiedensohler, A. Relationships between submicrometer particulate air pollution and air mass history in Beijing, China, 2004–2006. *Atmos. Chem. Phys.* **2008**, *8*, 6155–6168. [CrossRef]